Enhancement of the thermal conductive property of Epoxy via functional carbon nanotubes

Katsumi Yoshino, Toshiuki Ueno and Takashi Yoshioka

Shimane Institute for Industrial Technology,

Hokuryo-cho, Matsue, Shimane 690-0816 Japan

Wei Feng and Ning Dong

School of Materials Science and Engineering, Tianjin University, Tianjin 300072,

People's Republic of China

Abstract

Multiwalled carbon nanotubes (MWCNTs) were grafted by diphenyl methane diisocyanate (MDI) and the Epoxy resin separately. FT-IR and the Transmission Electron Microscopy (TEM) were used to provide the evidence of the grafting. Besaides, we took the two products and some assistant agent into curing and got the composites. In addition, we discussed the mechanical property, electronic property as well as the thermal property of the composite and worked on the Scanning Electron Microscopy (SEM) and TEM images, and reached up to the mechanisms of the content of carbon nanotubes, the carboxyl-terminated butadiene-acrylonitrile (CTBN) and the different process of the preparation and curing to get a goal of the best condition of the processing of the composite.

Key Words : Multiwalled carbon nanotubes; Diphenyl methane diisocyanate; Curing; Conductivenetwork

カーボンナノチューブによるエポキシ複合体の熱伝導特性の向上

吉野勝美[1)]、上野敏之[1)]、吉岡尚志[1)]　封　偉[2)]、董　宁[2)]

1) 島根県産業技術センター　690-0816 島根県松江市北陵町 1

2) 天津大学物質科学工学科　天津 300072　中華人民共和国

要旨

多層カーボンナノチューブをジフェニルメタンディイソシアネートとエポキシレジンにグラフトし複合体を作成し、機械的性質、電気的性質、熱的性質を測定し、特に熱的性質の著しい向上を明らかにした。

キーワード　多層カーボンナノチューブ、キュアリング、エポキシ、熱的性質

1. Introduction

Carbon nanotubes (CNTs) [1-3] have been drawn great attention ever since the discovery of them. The CNTs exhibit excellent mechanical properties[4], high thermal and electrical conductivity [5] as they are of a structure like crimp graphite. Epoxy (EP) is widely used in industrial fields for the good performance in mechanical, adhesive, technological and so forth. EP-based composites are extensively researched by researchers and a great number of works have dealt with CNT-reinforced EP [6-21]-to achieve a combination of the advantages of the two separately. There are works that indicate the relationship between the enhancement of both mechanical property and thermal and electrical conductivity and the CNTs contents.[6, 7] Generally speaking, improvements in interfacial adhesion as well as a good dispersion by nanotube functionalization have indicated the significant enhancement of mechanical properties [3, 8]. CNTs [9] have good potential to enhance the optoelectronic properties of conjugated polymers. CNTs are of a tailored structure which lead to a convenience to interact with conjugated polymers through the pep electronic interactions and when fillers have an aspect ratio of 10^3 which is a possible value obtainable for the case of single-walled carbon nanotubes, the expected percolation threshold is much less than 1 wt% as well[10]. In contrast, it is reported that this kind of composites show a low percolation threshold (<0.5 wt %) and an increase of more than 6 orders of magnitude in electrical conductivity, reaching values close to 10^{-2} S/m[11-14]. Sean et al [22] also prepared CNTs EP composites by the combination of surfactant and ultrasonication methods for suspending the single-walled carbon nanotubes (SWNTs) in a large amount of acetone, but no improvement in the modulus and compressive strength for a filament-wound composite with a 1 wt% nanotube addition was found. Microscopy showed a nonuniform dispersion of nanotubes in the EP. Kilbride *et al* [23] reported the conductivity behavior of the same system with a percolation threshold of 0.055 wt% of MWNTs but only very low conductivity of 1.4×10^{-7} S cm^{-1} for a composite containing 4.3 wt% MWNTs. Similar low conductivity value of approximately 5×10^{-7} S cm^{-1} was observed for a composite of poly (3-octylthiophene) containing 5 wt% SWNT. However, in this case the critical mass for percolation of 4 wt% was probably associated to SWNT bundling. Biercuk *et al* [24] reported a 125% thermal conductivity enhancement and an increase in Vickers hardness by a factor of 3.5 when 2 wt % SWNTs were added to the EP.

2. Experimental

2.5 g MWNTs were added into the mixture of 90 ml concentrated sulphuric acid and 30 ml concentrated nitric acid. The mixture of the three were put into the ultrasonic vibrations for 1.5 h and mechanically mixed for 3 h.

After ultrasonic vibrations, the mixture was refluxed for 2 h at 90℃, cooled down to room temperature and diluted with 200 ml of distilled water. The mixed acid was removed away by vacuum filtering with the 450 nm micro filtration membrane. Then the filter cake was washed with distilled water and centrifugalize at 4500 r/min for 15 min. The top suspension was collected. Retreat the deposit by centrifugalization for several times. The collected top suspension was vacuum filtered and the filter cake was dried, while the final deposit was recycled. 570 mg MWNTs-COOH was dried again in the vacuum drying chamber for 6 h.

Appropriate amount of calcium hydride was added into N,N-dimethylformamide (DMF). After stirred at room temperature for 36 h, the suspension was vacuum distillated and the distillates was the needed dried DMF. The prepared MWNTs-COOH was dispersed in DMF to form 5 wt % suspensions by using an ultrasonication for 1h. Diphenyl methane diisocyanate (MDI) solution in DMF of 5 wt% was added to the stirred suspension of MWNTs-COOH. The reaction was maintained at 80 °C under nitrogen for 1.5 h. The product was washed with DMF, water and acetone then dried in vacuum.

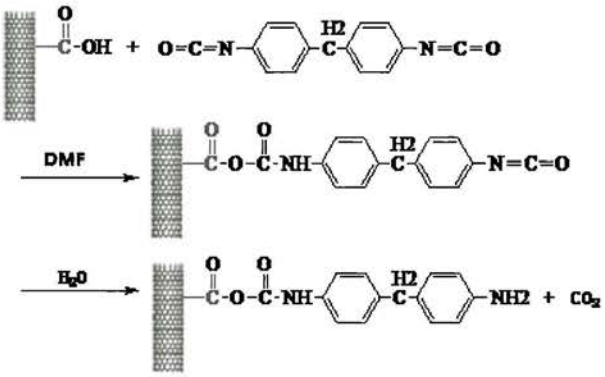

Schematic 1　Grafting of MWNTs and MDI

EP and MWNTs-COOH of 5 wt% was mixed in distilled water and treated with ultrasonic for 1h to get well dispersed. The mixture was stirred at 20 r/min and heated at 90℃ to get the distilled water out of the system. Then the well dispersed mixture was reacted at 140℃ for 6 hours.

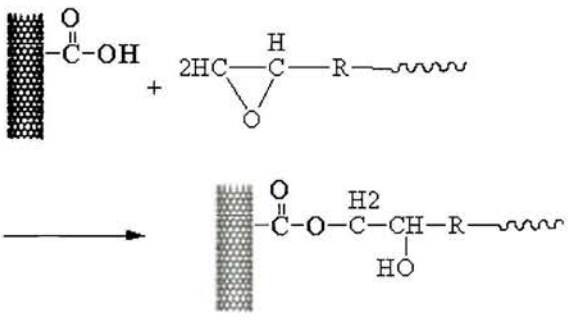

Schematic 2　Reaction between MWNTs and EP Resin

Table 1 Contents of the components in the samples

Sample Number	MDI-MWNTs/mg	EP-MWNT/mg	CTBA/mg	EMI/mg
1	50	500	200	50
2	100	500	200	50
3	200	500	200	50
4	100	500	250	50
5	100	500	150	50

In order to investigate the influence of the amount of MDI and carboxyl-terminated butadiene-acrylonitrile (CTBA) to the mechanic properties of final composite, we chose devise contents of the components to cure the composites, and the contents of components is listed in Table 1. The amount of MDI-MWNTs varies in the sample 1, 2, and 3, while the amount of CTBA changes in the sample 2, 4, and 5. The amounts of EP-MWNTs and 2-ethyl-4-methylimidazole (EMI), as the curing agent, are kept constantly in all the samples.

In the processing of the curing, we take use of two ways to mix the components to see which method is better. One is to mix through mulling, and the other is to mix the components in actone, undergo with the ultrasonic vibrations for 1 h to get a well disperse and put the mixture into vacuum to remove the acetone and bubbles. The temperature of the curing is at 80 ℃ forI h and 160 ℃ for 2h.The products of MDI-CNTs and the EP-CNTs were characterized by the Fourier transform infrared (FT-IR) spectra. The FT-IR spectra of MDI, MWNT-COOH as well as the EP were also carried on for the comparison

Three kinds of samples were prepared for the characteristic of the mechanical property of the curing product. As to the curing product bar, the size is of 50 mm×6 mm×1 mm. For the adhesive sample for the tensile-shear test, the area of the adhesive is of 8 mm×10 mm while for the adhesive sample for the tensile test the diameter is of 8 mm. In the tensile test, the tensile rate was set up as 1.00 mm/min.

The composites without curing were undergoing a differential scanning calorimetry (DSC) to study the curing process. Five different components of curing samples were sent to take a DSC test; the range of the temperature was from room temperature to 450℃. While the temperature range for the thermo gravimetry (TG) was from room temperature to 800℃.

The character of the thermal capacity and the thermal capacity were achieved through the thermal analyzerTA-50 with the samples of 10 mm×10 mm.

Scanning electron microscopy (SEM) images were taken with a PhilipsXL-30 at different acceleration voltages (1–1.5 kV). The samples were investigated of the nano-scaled reinforcements and allowing a contrast imaging of the fracture surfaces. Transmission electron microscopy (TEM) images were taken using a Hitachi-8000 at 120 kV. Ultra thin films of the composites (50 nm) were obtained by ultramicrotome cutting.

3. Results and discussion

3.1 The FT-IR spectra

The FT-IR spectra of MWNT-COOH, MDI and MDI-MNNTs are shown in Figure 1. The strong peak at 2270 cm^{-1} is the characteristic vibration of the –N=C=O in MDI. The peak at 3438 cm^{-1} in all the samples responds to the stretching vibration of the hydroxy group in the –COOH; The peak at 1659 cm^{-1} of MWNT-COOH indicates the stretching vibration of the C=O in the –COOH group. The absorption at 3310 cm^{-1} in MDI-MWNTs are corresponding to the asymmetrical stretching vibration of the N-H bond in the $-NH_2$ group; the 1649 $cm^{-1}$is the compound peak of the stretching vibration of the C=O both in the remnants –COOH group and the amido bond structure. The peaks at 1226 cm^{-1}, and 1529 cm^{-1} respond to the stretching vibration of the N-H, and the C-N in the amido bond separately which confirms the formation of the amido bond. All the signals demonstrate the MDI has been successfully combined to the MWNTs-COOH

The FT-IR spectra of MWNT-COOH, EP and EP-MWNTs are shown in Figure 2. The great absorption at between 800~1000 cm^{-1} is the characteristic peak of the 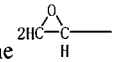 group in EP, The peak at 3410 cm^{-1} in both MWNT-COOH and EP-MWNTs responds to the stretching vibration of the hydroxy group in the –COOH; The peak at 1659 cm^{-1} of MWNT-COOH indicates the stretching vibration of the C=O in the –COOH group, the 1650 cm^{-1} is the compound peak of the stretching vibration of the C=O both in the remnants –COOH group and the amido bond structure. The absorption at around 3000 cm^{-1} of EP and EP-MWNTs are corresponding to the asymmetrical stretching vibration of the N-H bond in the $-NH_2$ group in the EP resin. The peaks at 1233 cm^{-1}, and 1534 cm^{-1} respond to the stretching vibration of the N-H, and the C-N in the amido bond separately which confirms the formation of the amido bond. In the spectrum of EP-MWNTs, the great absorptions at around 1780 cm^{-1} is correspond to the structure of 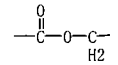 which is the evidence of the

successful grafting of EP resin and MWNTs-COOH yet the combination with carbon nanotubes has greatly reduced the content of the EP group.

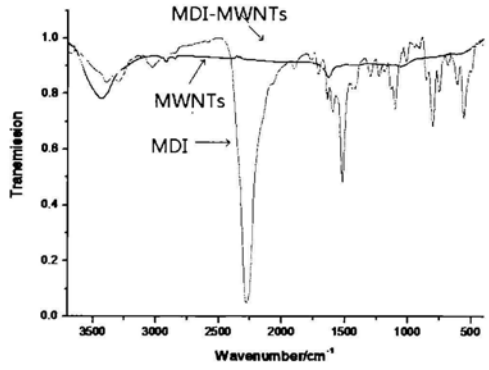

Figure1　FT-IR spectra of MDI and MDI-MWNTs

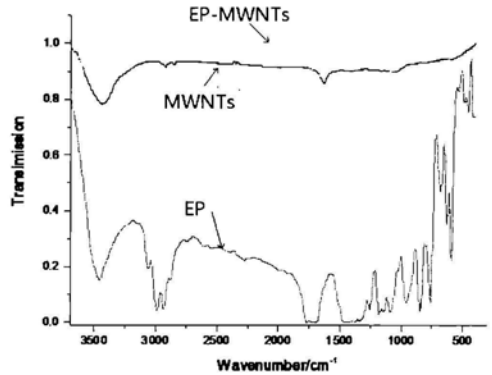

Figure 2　FT-IR spectra of EP and EP-MWNTs

3.2 The mechanical property

Figure 3 is the ε-σ curve for the composite with different content of MDI-CNTs and these samples were made through mulling. The curve of a, b and c corresponds to the sample number 1, 2 and 3 in the Table 1, respectively. We could see from the curves that as the content of MDI-MWNTs increases, the tensile strength of the composites shows an improvement which can reach up to 11 MPa. And the addition of the CTBA led to some toughness, because the curing product of the EP resin shows great brittleness and the dispersion of the MDI-MWNTs could hardly achieves the molecule level, which might result in the aggregation in the resin matrix and cause the stress concentration. It not only can result in the rupture performance, but also bring in great decrease of the tensile strength. However, the content of CTBA in the composite was limited as CTBA would decrease the thermal and electoral conductivity of the composite. However, the structure of MDI is of rigid and improves the strength of the composite.

Figure 4 is the ε-σ curve of the composite with different content of CTBA, and these sample were also made through mulling. The curve of a, b and c corresponds to the sample number 4, 2 and 5 in the Table 1, respectively. The bending performed as a trend that with increasing the amount of CTBA, the tensile strength of the composite decreases. That was because as the content of CTBA increases, the module of the composite goes down which could reform the stress concentration. However, as the cost of that the strength of the composite decreases that when the content of the CTBA equals half of the content of EP, the strength shows a sharp decrease to less than 10 MPa.

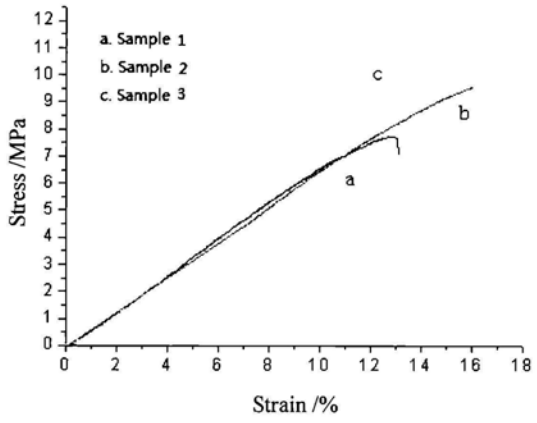

Figure 3　ε-σ curve of the composite with different content of MDI-CNTs

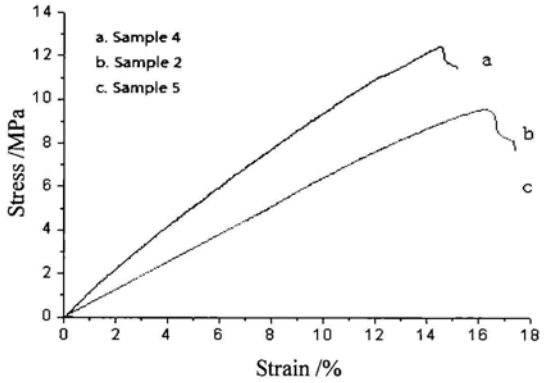

Figure 4　ε-σ curve of the composite with different content of CTBA

Figure 5 is the ε-σ curve of the composite achieved through different solvents. The content of component corresponds to the sample number 2 in Table 1. Curve a responds to the composite achieved from direct mulling while curve b and curve c are the composited achieved from ultra sonic treatment in DMF and acetone separately. It can be concluded that the samples of b and c exhibit higher tensile strength and better bending performance. That is because the ultra sonic treatment in solvents could lead to better dispersion, and the step of evaporating solvents as well as drying in vacuum can get rid of the bubbles in the composites which greatly reduce the stress concentration and improved the strength. Besides, the use of DMF as the solvent would lead to a better mixing of the composite

which can be conferred from the curves b and c, owning to the larger polarity of DMF, which facilitates the dispersion of the components in the system and makes the composites much more uniform in the microscopic degree and improve the mechanic property.

Figure 6 is the tensile-shear curve of the adhesive all the samples made through mulling, and the curves a, b, c, d and e corresponds to the sample number listed in Table 1. From curves a, b and c, it can be concluded how the content of MDI-MWNTs affects the tensile-shear strength. As the content of MDI-MWNTs increases, the tensile-shear strength increases. That is because the rigid structure in the MDI molecule helps to improve the strength and the fabric structure of MWNTs wrapped by MDI can reinforce the composite. In addition, the more the MDI-MWNTs in the system, the more fragile the composites is, which is because of the increase of the rigid structure, and the more the MDI-MWNTs lies in the composite, the worse the disperse of that, causing the stress concentration. In the figure 6, the curves of b, d and e shows how the content of CTBA works on the strength of the composite. Through the comparison of the three curves, we could see that CTBA brings in better bending but lowers the strength.

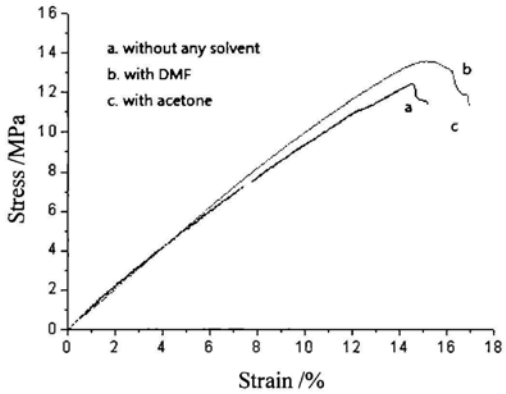

Figure 5 ε-σ curve of the composite through different solvants

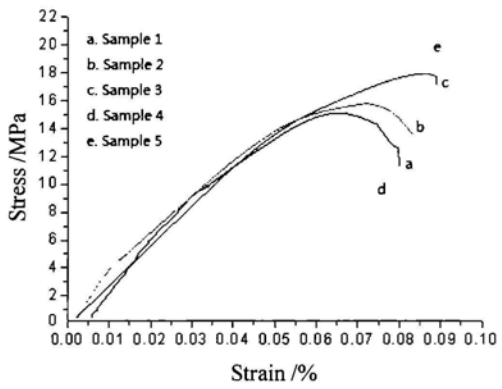

Figure 6 tensile- shear curve of the achieved adhesive sample

3.3 The thermal properties

Figure 7 is the DSC curve of the curing course under different rate of temperature rising. In the course of curing, curing reaction could take place at the very beginning of the temperature rising, and the peak of the curing temperature lies at around 130℃ to 170℃. As the rate of temperature rising, the time for curing become shorter and the curing peak become extent. That is because when the rate of temperature rising, the transformation of enthalpy tends to be more which leads to a larger thermal interia and the curing heat release peak moves to higher temperature. In the composite, according to the temperature rising rate, the ending temperature lies at about 200℃.

Figure 8 is the TG curve of the curing composites to see the thermal resistance and the curves a, b, c, d and e corresponds to the sample number listed in Table 1. The first weight loss lies at 450℃-500℃ and it indicates an remarkable thermal decompose during which the loss reach up to 50% and according to the contents of the components, the weight loss respond to the CTBA and EP that are not so well reacted.

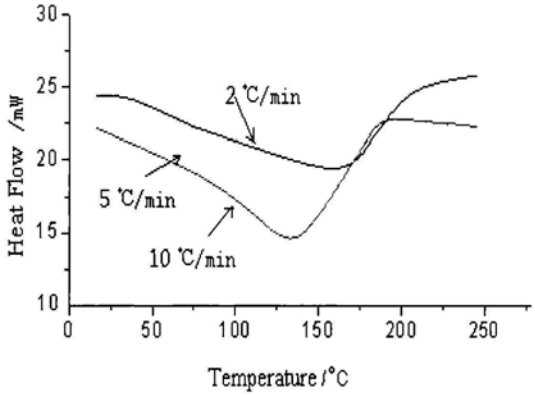

Figure 7 DSC under different ratio of temperature rising

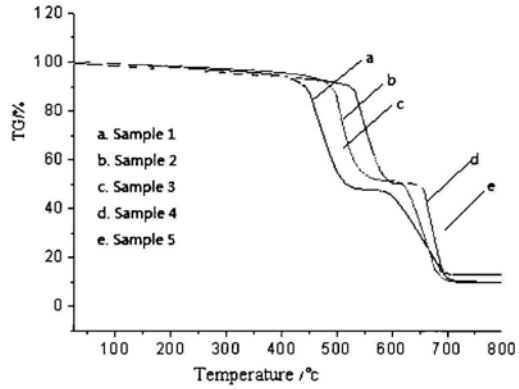

Figure 8 TG of the curing composite

In Figure 9, curve a and b are separately the thermal capacity and the thermal conductivity of the composite impacted by the content of the MDI-MWNTs. It can be concluded from the figure that the EP is of very low thermal conductivity which is at about 0.21 W/mK and as the content of the MDI-CNTs increases, the thermal conductivity of the composites shows a remarkable increase. At first it is because of the conductive network was formed to some extent when the content of MWNTs increased in the whole composite and the rigid structure of MDI did good to the vibrating thermal conductivity, which lead to a much more adjustable vibration of the molecule and a faster conduction of thermal. In addition, the volume contraction during the curing can decrease the distance between MWNTs, the MDI molecules, which promotes the formation of the conductive network. It is needed to be mentioned that the dispersion of MWNTs has to be improved and if an identical orientation is achieved, the thermal conductivity will get a much tremendous increase.

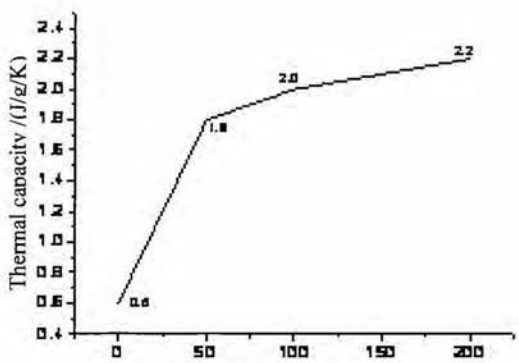

a

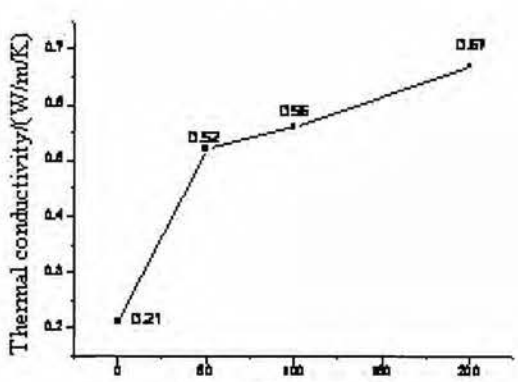

b

Figure 9 Thermal capacity (a) and thermal conductivity (b) of the composite impacted by the content of the MDI-CNTs

Figure 10 is the thermal capacity and the thermal conductivity of the composite impacted by the content of the CTBA separately. It can be seen from the figure that as the content of CTBA rises the thermal conductivity shows a sharp down tendency. That is because the CTBA molecules don't have the thermal conductivity through electron thermal conductive mechanism like the metal and the conductive polymers, so the efficiency of the phonon thermal conductive is very low as the structure of CTBA is loose and soft. As the result, the more CTBA exist in the composite, the larger the content of the soft structure is. The soft part in the composite greatly reduces the thermal capacity and the thermal conductivity of the composites.

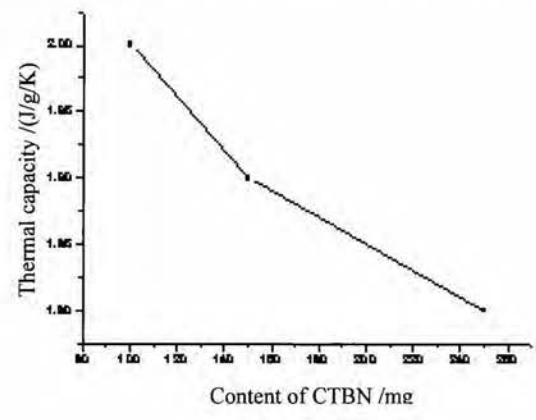

a

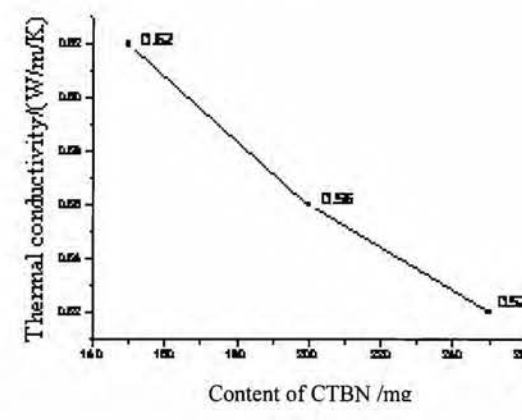

b

Figure 10 Thermal capacity (a) andthermal conductivity (b) of the composite impacted by the content of the CTBA

3.4 The SEM and TEM

Figure 11 is the SEM image of MDI-MWNTs, from which we can see the outside of MWNTs have been warpped by MDI and the sample takes on a state of fleecy. Corresponding to the FT-IR, the MDI has been successfully connected to the side wall of MWNTs.

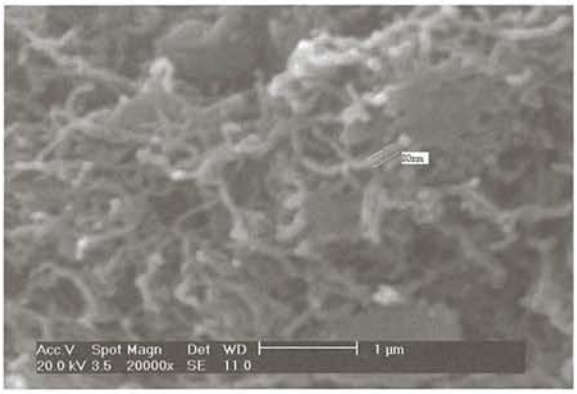

Figure 11 SEM of the MDI grafted MWNTs

Figure 12 are the SEM images for the composites achieved through mulling (a) and ultrasonic dispersion in DMF (b) and the content of components is corresponding to the sample 2 listed in Table 1. By the comparison of the two samples, amounts of bubbles can be found in (a), which was given birth to during the mulling, and the larger viscosity made the wiping off of the bubble through heating useless. The bubbles would act as the stress concentration spot and let down the strength of the composite. Meanwhile the existence of the bubbles would also block the formation of the conductive net work.

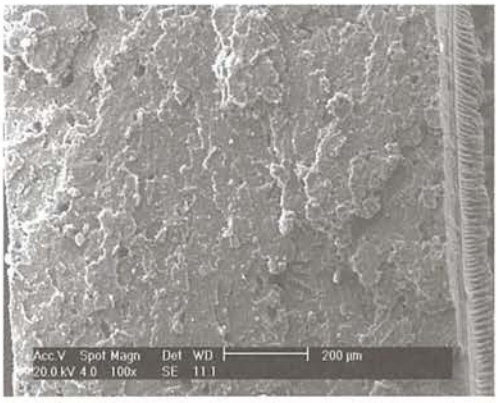

a

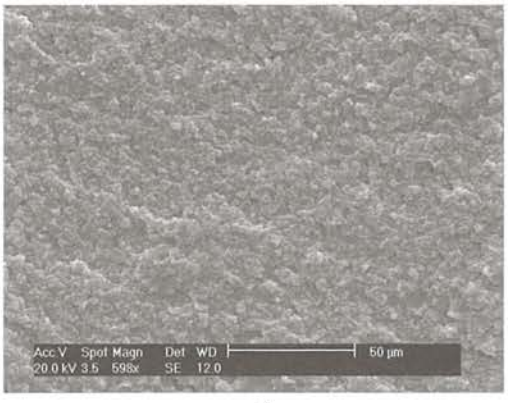

b

Figure 12 SEM images of the composites through mulling a) and ultrasonic dispersion b).

Figure 13 are the TEM images of the curing samples 2 listed in Table 1 through ultrasonic dispersion in DMF solution. In figure, the MDI modificated has a good compatibility with the EP resin. That is because the diisocyanate in the MDI has turned in to the amido which has great polarity and can combine with EP resin closely. Therefore, a better dispersion of MWNTs in the EP resin can finally be realized.

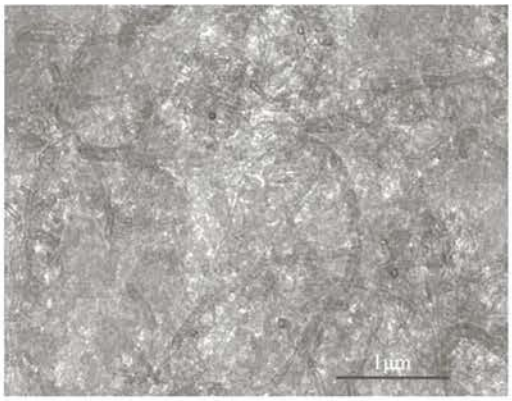

Figure 13 TEM images of the curing samples

4. Conclusions

MWNTs were grafted by MDI and EP resin separately. FT-IR spectra and TEM were used to provide the evidence of the grafting of MDI on MWNTs and the combination of MWNTs and EP. Mechanical property of the composite test informed that the MWNTs-MDI could improve the tensile strength, while the CTBA can improve the toughness. The thermal conductivity of the materials was improved via the introduction of carbon nanotubes into the molecular structure.

References

[1] Iijima S. Helical .Nature 1991(354):56.
[2] Oberlin A, Endo M. J Cryst Growth 1976(32): 335.
[3] Nesterenko AM, Kolesnik NF, Akhmatov YS, Sukhomlin VI, Prilutski OV. Metals 3 UDK 869.173.23. News of the Academy of Science, USSR,1982(12):6.
[4] Thostenson ET, Ren Z, Chou TW. Compos Sci Technol 2001(61):1899.
[5] Berber S, Kwon YK, Toma´nek D. Phys Rev Lett 2000(84):4613.
[6] Jiang Z, JongD K, Hai Q P, John L. M, Valery N. K, and Enrique V. B. Nano Letters. 2003(3): 1107.
[7] Bal. S and Samal S.S.. Bull. Mater. Sci. 2007(30):379.
[8] Gojny F. H., Wichmann M. H. G., Fiedler B., Schulte K. Compos Sci Technol 2005(65): 2300.
[9] Cahill DG, Goodson K, Majumdar A. J Heat Transfer 2002(124): 223.

[10] Biercuk, MJ, Llaguno, M, Radosavljevic, M, Hyun, JK, Johnson AT, Fischer JE. Appl Phys Lett 2002(80): 2767.
[11] Barrau, S., Demont, P., Peigney, A., Laurent, C., Lacabanne, C. Macromolecules. 2003(36): 5187.
[12] Bryning, M. B., Islam, M. F., Kikkawa, J. M., Yodh, A. G. AdvMater 2005(17): 1186.
[13] Gojny, F. H., Wichmann, M. H. G., Fiedler, B., Kinloch, I. A.,Bauhofer, W., Windle, A. H., Schulte, K. Polymer 2006 (47): 2036.
[14] Li, N., Huang, Y., Feng, D., Xiabo, H., Xiao, L., Gao, H.,Ma, Y., Li, F., Chen, Y., Eklund, P. C. Nano Lett 2006 (6): 1141.
[15] Valentini, L., Puglia, D., Frulloni, E., Armentano, I., Kenny, J. M., Santucci, S. Compos Sci Technol 2004 (64): 23.
[16]Sandler, J. K. W., Kirk, J. E., Kinloch, I. A., Shaffer, M. S. P.,Windle, A. H. Polymer 2003(44): 5893.
[17] Wang, Z., Liang, Z. Y., Wang, B., Zhang, C., Kramer, L. Compos A 2004 (35): 1225.
[18] Liao, Y.H., Marietta-Tondim, O., Liang, Z., Zhang, C., Wang, B. Mater Sci Eng A 2004(385): 175.
[19] Lau, K.T., Lu, M., Lam, C.K., Cheug, H.Y., Sheng, F.L., Li, H.L. Compos Sci Technol 2005(65): 719.
[20] Zhu, J., Peng, H., Rodriguez-Macias, F., Margrave, J. L., Khabashesku, V. N., Imam, A. M., Lozano, K., Barrera, E. V. Adv Funct Mater 2004(14):643.
[21]Yuen, S.M., Ma, C.C. M., Wu, H.H., Kuan, H.C., Chen, W.J., Liao, S.H., Hsu, C.W., Wu, H.L. J Appl Polym Sci 2007(103): 1272.
[22] Spindler-Ranta, S., Bakis, C. E. SAMPE 2002 Symposium &Exhibition, 2002.
[23] Gustavsson M, Karawacki E, Gustafsson SE. Rev Sci Instrum 1994 (65):3856.
[24] Biercuk, M. J., Llaguno, M. C., Radosavljevic, M. Appl. Phys. Lett. 2002(80): 2767.

(October 15, 2011 Accepted)